

## ESO Phase 3 Data Release Description

<b>Data Collection</b>	<i>KiDS</i>
<b>Release Number</b>	2
<b>Data Provider</b>	Konrad Kuijken
<b>Date</b>	14.11.2014

### Abstract

This data release constitutes the second public release by the Kilo-Degree Survey (KiDS). KiDS is an ESO public survey carried out with the VLT Survey Telescope and OmegaCAM camera, that will image 1500 square degrees in four filters (u, g, r, i), in single epochs per filter. KiDS is designed to be a weak lensing shear tomography survey, and has as its core science drivers mapping of the large-scale matter distribution in the universe and constraining the equation-of-state of Dark Energy. Secondary science cases are manifold and range from galaxy evolution to Milky Way structure, and from detection of white dwarfs to high-redshift quasars.

This second data release can be considered an incremental release. In this release the same types of data products are provided as in the first data release for an additional set of survey tiles (calibrated, stacked images and their weights, as well as masks and single-band source lists extracted from the stacks). Apart from that, a different type of data product (a multi-band source catalogue) is provided that encompasses the combined area of the data releases 1 and 2. Together, these data releases cover the first 148 square degrees that were observed in all filters. The data were taken under ESO programme IDs: 177.A-3016(A), 177.A-3016(B), 177.A-3016(C), 177.A-3016(D), 177.A-3016(G), 177.A-3017(A).

### Overview of Observations

This data release (KiDS-ESO-DR2) consists of the coadded images, weight maps, masks and source lists of the 98 tiles that were completed (i.e. the final data for the tile was obtained) between 1 October 2012 and 31 September 2013, adding to the 50 survey tiles released in KiDS-ESO-DR1. Furthermore, KiDS-ESO-DR2 contains a multi-band source catalogue encompassing these tiles, as well as the tiles included in the first data release (KiDS-ESO-DR1), a total of 148 survey tiles. Figure 1 shows the locations of these tiles within the KiDS fields. Partial observations for many of the other fields exist as well and will be included in future releases once their wavelength coverage is complete.

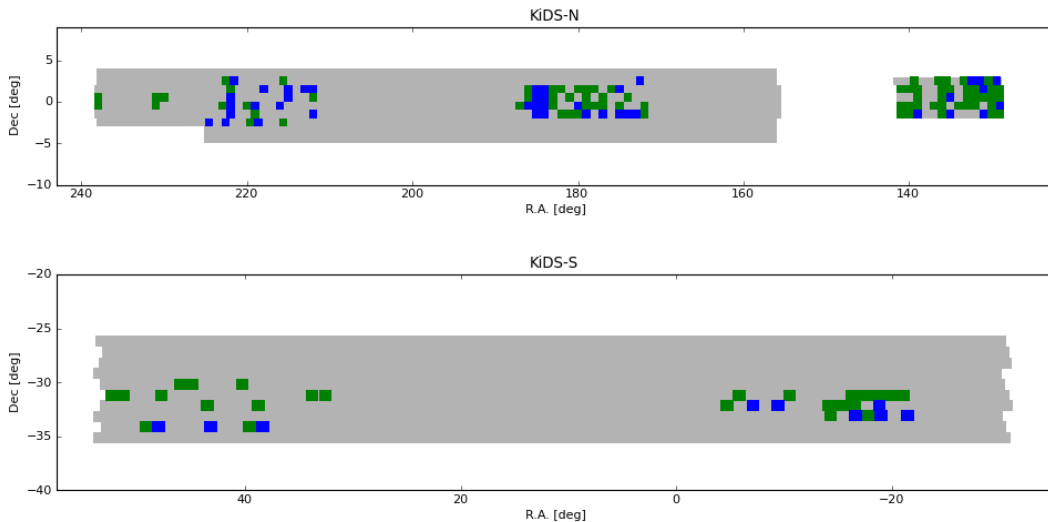


Figure 1: location of the 50 KiDS-ESO-DR1 tiles (blue) and the 98 KiDS-ESO-DR2 tiles (green); the two KiDS fields (top: KiDS-North; bottom: KiDS-South) are outlined in grey.

## Release Content

### Imaging products and single-band source lists

The complete list of 98 tiles for which imaging data products and single-band source lists are included in KiDS-ESO-DR2 is provided online: [http://kids.strw.leidenuniv.nl/DR2/data\\_table.php](http://kids.strw.leidenuniv.nl/DR2/data_table.php)

Each tile was observed in u, g, r, and i band. The final footprint of each tile is slightly larger than 1 square degree due to the dithering scheme: 61.9x65.4 arcminutes in u; 62.3x66.8 arcminutes in g, r and i. Taking this into account, the total sky coverage is approximately 107 square degrees, which is not contiguous, as illustrated in Figure 1.

The single-band source lists were extracted from the calibrated, stacked images for each tile and filter separately.

Since the OmegaCAM CCD mosaic consists of 32 individual CCDs, the sky covered by a single exposure is not contiguous but contains gaps. In order to fill in these gaps, KiDS tiles are built up from 5 dithered observations in g, r and i and 4 in u. The dithers form a staircase pattern with dither steps of 25'' in X (RA) and 85'' in Y (DEC), bridging the inter-CCD gaps (de Jong et al., 2013, ExA 35, 25). The tile centers are based on a tiling strategy that tiles the full sky efficiently for VST/OmegaCAM. Neighbouring dithered stacks have an overlap in RA of 5% and in DEC of 10%.

Exposure times and observing constraints for the four filters are tabulated in Table 1.

Filter	Max. FLI	Min. moon distance	Max. seeing (arcsec)	Max. airmass	Sky transp.	Dithers	Total Exp. time (s)
u	0.4	90	1.1	1.2	CLEAR	4	1000
g	0.4	80	0.9	1.6	CLEAR	5	900
r	0.4	60	0.8	1.3	CLEAR	5	1800
i	1.0	60	1.1	2.0	CLEAR	5	1080

Table 1: KiDS observing strategy; observing condition constraints in place for KiDS-ESO-DR2, exposure times, and number of dithers for each filter.

In Figure 1 the obtained seeing (FWHM), PSF ellipticity, and limiting magnitude ( $5\sigma$  AB in 2'' aperture) distributions per filter are shown, to illustrate the obtained data quality. In case of the filters observed in dark time (u, g, r) the FWHM distributions reflect the different observing constraints, with r-band taking the best conditions. Since i-band is the only filter observed in bright time, it is observed under a large range of seeing conditions. Average PSF ellipticities are always small:  $<0.1$  (the average is over the absolute amount of ellipticity, regardless of the direction of ellipticity). The wide range of limiting magnitudes in i-band is caused by the large range in moon phase and thus sky brightness.

For a full overview of the data quality parameters for each observation we refer to the following online table: [http://kids.strw.leidenuniv.nl/DR2/data\\_table.php](http://kids.strw.leidenuniv.nl/DR2/data_table.php)

This part of the data release consists of 392 files and a total data size of 1.4 TB.

### Multi-band source catalogue

Also included in KiDS-ESO-DR2 is a multi-band source catalogue. This source catalogue is based not only on the imaging data products described above, but also encompasses the tiles released in the first data release of KiDS (KiDS-ESO-DR1). Here we provide a general description of the catalogue data, while an overview of all tiles with coordinates, PSF size, limiting magnitude, etc. is provided online: [http://kids.strw.leidenuniv.nl/DR2/catalog\\_table.php](http://kids.strw.leidenuniv.nl/DR2/catalog_table.php)

The catalogue is based on a total of 148 survey tiles, providing a total area coverage of approximately 160 square degrees. As illustrated in Figure 1 the area covered is very patchy. As a result, no global photometric or astrometric calibration of the catalogue is possible and all photometry is therefore done per tile. Zeropoint offsets w.r.t. SDSS are calculated for all tiles in KiDS-North and also provided in the table linked above.

Figure 2 shows the PSF sizes, average ellipticities and limiting magnitudes for all tiles included in the catalogue. As for the imaging products the overall image quality is best in r-band. For this reason the r-band data were used for the object detection for the catalogue. Subsequently, SEX-

tractor was run in double-image mode to measure source parameters in the other filters. The star-galaxy classification included in the catalogue is also based on the r-band data.

The catalogue contains a total of 16,779,053 sources and is made up of 149 files (148 data files and 1 metadata file) with a total data volume of 11 GB.

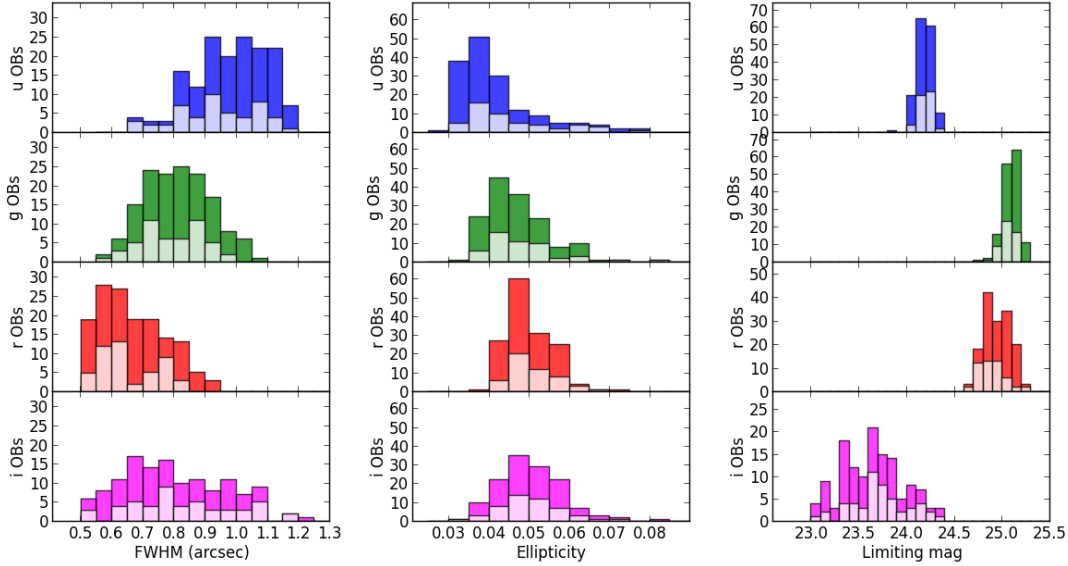


Figure 2: obtained raw data quality parameters for KiDS-ESO-DR1 and KiDS-ESO-DR2. The white portions of the histograms correspond to the 50 tiles in KiDS-ESO-DR1 and the colored portions to the 98 tiles newly released in KiDS-ESO-DR2; the multi-band catalogue combines all 148 tiles and therefore corresponds to the total histograms. **Left:** average PSF size (FWHM) distributions; **center:** average ellipticity distributions; **right:** limiting magnitude distributions ( $5\sigma$  AB in  $2''$  aperture). The distributions are per filter: from top to bottom u, g, r, and i, respectively.

## Release Notes

### Data Reduction and Calibration

The KiDS-ESO-DR2 pipeline, with the exception of the creation of the multi-band catalogue, is identical to the KiDS-ESO-DR1 pipeline and based on the Astro-WISE optical pipeline described in McFarland et al. (2013, ExA 35, 79) (MF13). Below we summarize the processing steps and list KiDS-specific information (i.e., KiDS process configuration and departures from Astro-WISE optical pipeline).

#### Image detrending

Detrending of the raw data consists of the following steps.

- **Cross-talk correction.** Electronic cross-talk occurs between CCDs #93, #94, #95 and #96, resulting in faint imprints of bright sources on neighbouring CCDs. A correction was made for cross-talk between CCDs #95 and #96, where it is strongest (up to 0.7%).
- **De-biasing and overscan correction.** First, for each science and calibration exposure the overscan is subtracted per row (using method 6, see MF13). Second, a daily overscan-subtracted bias is subtracted. This is a daily average of 10 biases with  $3\sigma$ -rejection.
- **Flat-fielding.** A single masterflat (per CCD and filter) was used for all data in the release. This is by virtue that the intrinsic pixel sensitivities can be considered constant to  $\sim 0.2\%$  or better for g, r and i (Verdoes Kleijn et al., 2013, ExA, 35, 103). For g, r and i this master flat is a combination of a master dome (for high spatial frequencies) and master twilight (=sky) flat-field (for low spatial frequencies). Both contributing flats are an average of 5 raw flat-field exposures with  $3\sigma$ -rejection. In u band only the twilight flats are used.

- **Illumination correction.** Illumination correction (a.k.a. “photometric superflat”) is applied *in pixel space*, and only on the source fluxes (i.e., after background subtraction). A single illumination correction image is used to correct the single master flats per filter for all KiDS-ESO-DR2 data (see Verdoes Kleijn et al., 2013, ExA 35, 103).
- **De-fringing.** De-fringing is only needed for KiDS i-band. Analysis of nightly fringe frames showed that the pattern is constant in time. Therefore, a single fringe image was used for all KiDS-ESO-DR2 images observed after 2012-01-11. For each science exposure this fringe image is scaled (after background subtraction of the science exposure and fringe frame) and then subtracted to minimize residual fringes.
- **Pixel masking.** Cosmic-rays, hot and cold pixels, saturated pixels are automatically masked as described in MF13 during de-trending. These are included in the weight image. Additional automatic and manual masking is applied on the coadds (see below).
- **Satellite track removal.** Satellite tracks are detected automatically by applying the Hough transform (Hough, 1962) to a difference image of maximally overlapping exposures within a dither sequence after masking bright stars and bright ghosts. The pixels affected by satellite tracks are masked and included in the weight image.
- **Background subtraction.** To remove vignetting by bond wire baffling (Iwert et al. 2006, Proc. SPIE 6276, 62760A) in the focal plane, a row-by-row background subtraction method is used, before the background subtraction done by SWARP (see below).

### Photometric calibration

The steps taken to calibrate the photometry are as follows.

- KiDS-ESO-DR2 photometric calibration starts with individual zero points per CCD based on SA field observations. The calibration deploys a fixed aperture (6.3 arcsec diameter) not corrected for flux losses, and uses SDSS DR8 PSF magnitudes of stars in the SA fields as reference. Magnitudes are expressed in AB in the instrumental photometric system (i.e., no color corrections between OmegaCAM and SDSS photometric system applied).
- Next, the photometry in the g, r, and i filters is homogenized across CCDs and dithers for each filter in each tile independently. For u-band this homogenization is not applied because the relatively small source density often provides insufficient information to tie adjacent CCDs together. This global photometric solution is derived and applied in three steps:
  1. From the overlapping sources across dithered exposures, zero point differences between the dithers (e.g. due to varying atmospheric extinction) are derived.
  2. Zero point differences across CCDs are calculated using all CCD overlaps between the dithered exposures. Steps 1 and 2 both apply a minimization algorithm (see Maddox et al. 1990, MNRAS, 246, 433).
  3. The zero point offsets are applied to all CCDs w.r.t. an average zero point valid for the night, derived from the nightly SA field observations. If no SA field observations are available for the night, default values are used instead.

### Astrometry, regridding and coadding

A global (multi-CCD and multi-dither) astrometric calibration is calculated per filter per tile. SCAMP (Bertin 2006, ASP Conf. Series 351, 112) is used for this purpose, with a polynomial degree of 2 over the whole mosaic. The (unfiltered) 2MASS-PSC (Skrutskie et al. 2006, AJ, 131, 1163) is used as astrometric reference catalogue. A more detailed description of the astrometric pipeline is in MF13.

SWARP is used to resample all exposures in a tile to the same pixel grid, with a pixel size of 0.2 arcseconds. After background subtraction the exposures are coadded using a weighted mean stacking procedure.

### Masking of bright stars and defects

A stand-alone program dubbed Pulecenella v1.0 (Huang et al. 2013, in prep.) was developed to create masks for KiDS coadds. It is an automatized procedure for mask creation completely independent from external star catalogues. An example of a detail of a mask is shown in Figure 3. Pulecenella detects the following types of critical areas, all related to bright stars:

- saturated pixels,
- spikes caused by diffraction by the mirror supports,
- readout spikes,
- reflection halos produced by the optics components (a central core halo, and up to three wider reflection halos with spatially dependent offsets, depending on the brightness of the star).

Defects that are not related to bright stars, such as satellite tracks (if missed by automated masking during de-trending) or other artifacts, are not detected by Pulecenella; for KiDS-ESO-DR2 coadds these areas have been masked by hand and included in the final masks.

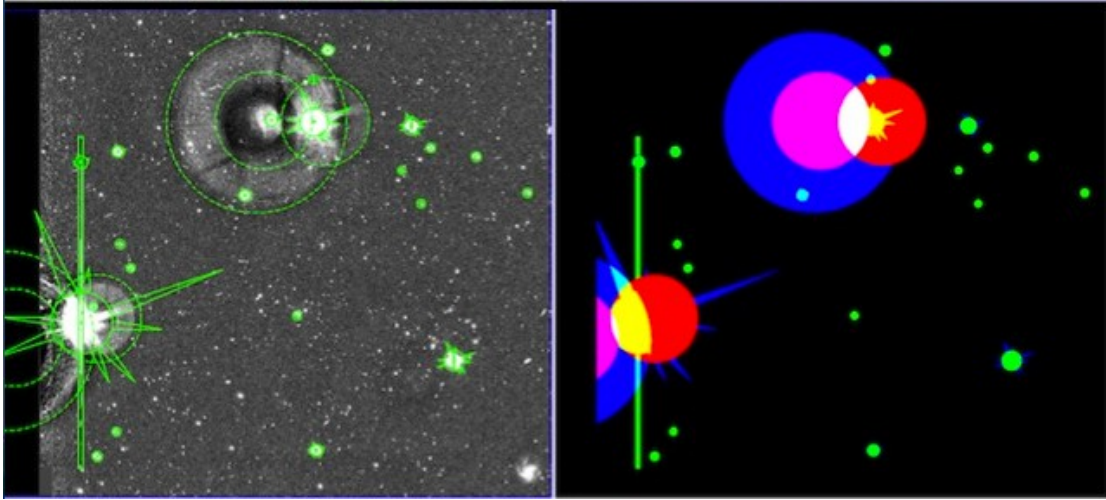


Figure 3: Detail of a Pulecenella v1.0 mask. **Left:** detail of a KiDS stacked image with bright stars; critical areas detected by Pulecenella are overplotted with green outlines. **Right:** FLAG image corresponding to the image shown on the left, with different colors indicating the pixel values resulting from the combination of different flag values.

The masks are provided as FITS FLAG images, where each type of critical region is identified by a different flag value, as listed in Table 2. During source extraction for the single-band source list (see below) the FLAG image is used to flag sources whose isophotes overlap with the critical areas. The resulting flags are stored in the following two source parameters:

- IMAFLAGS\_ISO: FLAG image flags OR'd over the isophote profile
- NIMAFLAG\_ISO: number of flagged pixels entering IMAFLAGS\_ISO

Type of area	Flag value	Type of area	Flag value
Readout spike	1	Secondary halo	16
Saturation core	2	Tertiary halo	32
Diffraction spike	4	Bad pixel	64
Primary halo	8	Manually masked region	128

Table 2: Critical areas in the masks and their flag values.

#### Single-band source list extraction and star/galaxy separation

The single-band source lists delivered in this data release are intended as “general purpose” source lists. Source list extraction and star/galaxy (hereafter S/G) separation is done with an automated stand-alone procedure optimized for KiDS data: KiDS-CAT. This procedure, the backbone of which is formed by S-Extractor (Bertin & Arnouts, 1996, A&AS, 317, 393) performs the following steps.

1. S-Extractor is run on the stacked image to measure the FWHM of all sources. High-confidence star candidates are then identified (for details see La Barbera et al. 2008, PASP, 120, L681).
2. The average PSF FWHM is calculated by applying the bi-weight location estimator to the

- FWHM distribution of the high-confidence star candidates.
3. A second pass of S-Extractor is done with SEEING\_FWHM set to the derived average PSF FWHM. During this second pass the image is background-subtracted, filtered and thresholded “on-the fly”. Detected sources are then de-blended, cleaned, photometered, and classified. A number of S-Extractor input parameters are set individually for each image (e.g., SEEING\_FWHM and GAIN), while others have been optimized to provide the best compromise between completeness and spurious detections (see Data Quality section below). The detection set-up used is summarized in Table 3; a full S-Extractor config file is available at this URL: [http://kids.strw.leidenuniv.nl/DR2/example\\_config.sex](http://kids.strw.leidenuniv.nl/DR2/example_config.sex)  
Apart from isophotal magnitudes and Kron-like elliptical aperture magnitudes, a large number of aperture fluxes are included in the source lists. This allows users to estimate aperture corrections and total source magnitudes. All parameters provided in the source lists are listed in the Data Format section below.
  4. S/G separation is performed based the CLASS\_STAR (star classification) and SNR (signal-to-noise ratio) parameters provided by S-Extractor and consists of the following steps:
    - In the SNR range where the high-confidence star candidates are located (the red dots in Figure 4) the bi-weight estimator is used to define their CLASS\_STAR location,  $\theta$ , and its width,  $\sigma$ ; a lower envelope of  $\theta - 4\sigma$  is defined.
    - At SNR below that of the high-confidence star candidates, a running median CLASS\_STAR value is computed from sources with CLASS\_STAR > 0.8, which is shifted to match the  $\theta - 4\sigma$  locus. The resulting curve (blue curve in Figure 4) defines the separation of stars and galaxies.

The source magnitudes and fluxes in the final source lists are not corrected for Galactic foreground or intergalactic extinction. The result of the S/G classification is available in the source lists via the 2DPHOT flag. Flag values are: 1 (high-confidence star candidates), 2 (objects with FWHM smaller than stars in the stellar locus, e.g., some cosmic-rays and/or other unreliable sources), 4 (stars according to S/G separation), and 0 otherwise (galaxies); flag values are summed, so 2DPHOT = 5 signifies a high-confidence star candidate that is also above the S/G separation line.

Additional information, and source lists with alternative detection set-ups can be found on the following website: <http://kids.strw.leidenuniv.nl/DR2/>

Parameter	Value	Description
DETECT_THRESH	1.5	<sigmas> or <threshold>,<ZP> in mag.arcsec <sup>-2</sup>
DETECT_MINAREA	3	minimum number of pixels above threshold
ANALYSIS_THRESH	1.5	<sigmas> or <threshold>,<ZP> in mag.arcsec <sup>-2</sup>
DEBLEND_NTHRESH	32	Number of deblending sub-thresholds
DEBLEND_MINCONT	0.001	Minimum contrast parameter for deblending
FILTER	Y	Apply filter for detection (Y or N)
FILTER_NAME	default.conv	Name of the file containing the filter
CLEAN	Y	Clean spurious detections? (Y or N)?
CLEAN_PARAM	1.0	Cleaning efficiency
BACK_SIZE	256	Background mesh: <size> or <width>,<height>
BACK_FILTERSIZE	3	Background filter: <size> or <width>,<height>
BACKPHOTO_TYPE	LOCAL	can be “GLOBAL” or “LOCAL”
BACKPHOTO_THICK	24	thickness of the background LOCAL annulus

Table 3: detection set-up for KiDS-ESO-DR2 single-band source lists

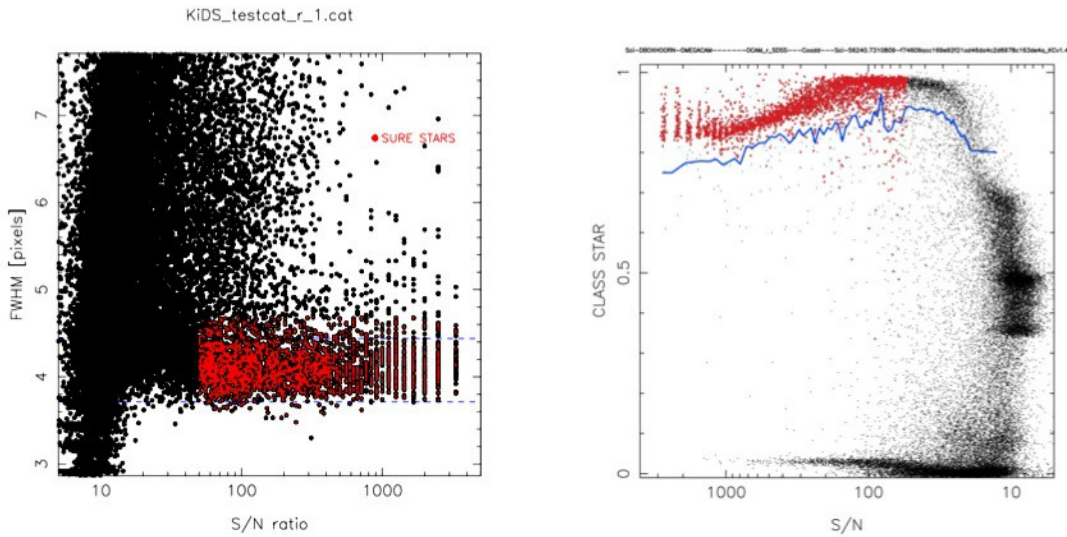


Figure 4: High-confidence star candidates and star/galaxy separation. **Left:** the high-confidence star candidates (red dots) are used to locate the stellar locus and calculate the average FWHM of the image. **Right:** example of star/galaxy separation; at  $SNR > 50$ , the high-confidence star candidates (red dots) are used to define the blue line; at lower SNR, all sources with  $CLASS\_STAR > 0.8$  are used; sources above the blue line are classified as stars.

### Multi-band source catalogue

The multi-band source catalogue delivered in this data release is intended as “general purpose” catalogue. The source parameters included in the catalogue are based on double-image mode runs of S-Extractor, where the r-band coadd of each tile is used as detection image and the detection set-up is identical to that used for the single-band source lists (Table 3). Since the r-band image is on average the best quality image for each tile, the S/G separation provided in the catalogue is the same as in the r-band single-band source list. The same masking flags (Table 2) are also included, for each filter. The source magnitudes and fluxes in the catalogue are not corrected for Galactic foreground or intergalactic extinction.

Seeing differences between filters are accounted for by aperture corrections. These aperture corrections have been calculated for each filter by comparing the flux in the aperture magnitudes included in the catalogue with the flux in a 6 arcsecond aperture, which is the aperture size used for photometric calibration. The resulting aperture corrections are applied to create the aperture-corrected fluxes included in the catalogue.

To prevent sources in tile overlaps from appearing multiple times in the catalogue, the survey tiles have been cropped to seamlessly connect to each other. This means that along the edges of survey tiles the data are less deep, but no worse than in the areas located in the gaps between the rows of CCDs in the focal plane.

## Data Quality

### Photometric quality

The matter of photometric quality can be split up in two:

1. the uniformity of the photometry within each tile
2. the quality of the absolute photometric calibration per tile/filter

Unfortunately, the distribution of tiles included in KiDS-ESO-DR2 is not contiguous, with many isolated tiles. Because of this, a complete homogenization of the photometric calibration for the entire data set was not possible. This should improve greatly in future releases.

Both the internal photometric homogeneity within a coadd and the quality of the absolute photometric scale is assessed by comparing the KiDS-ESO-DR2 photometry to SDSS DR8 (Aihara et al., 2011, ApJS, 193, 29). For this, PSF magnitudes were extracted from SDSS DR8 and compared to

the aperture-corrected magnitudes in the KiDS-ESO-DR2 multi-band catalogue. Only stars with photometric errors both in KiDS and in SDSS smaller than 0.02 mag in g, r, and i or 0.03 in u were used. This comparison can be done only for all tiles in the KiDS-North field, but since KiDS-South was calibrated in the same way as KiDS-North, we expect the conclusions to hold for all data.

The quality of the absolute photometric scale is illustrated in the left panels in Figure 5, where the distributions of photometric offsets between KiDS and SDSS are shown for the overlapping tiles in the KiDS-North field. A systematic offset of  $\sim 0.02$  mag is present in all filters. This could be due to the fact that nightly zero points are determined using a fixed aperture on stars in the SA field without aperture correction. The scatter and occasional outliers are due to non-photometric conditions (during either KiDS or SA field observations) and, particularly in case of the u-band, use of default zero points for nights without good SA field observations. The quality of this absolute photometry will improve greatly in future releases with significant contiguous area, which will allow a global calibration for the entire survey. All zero point offsets determined from this comparison with SDSS are available in the following online table:

[http://kids.strw.leidenuniv.nl/DR2/catalog\\_table.php](http://kids.strw.leidenuniv.nl/DR2/catalog_table.php)

Figure 6 shows the offsets between KiDS and SDSS DR8 magnitudes for 1 tile (KIDS\_129.0\_-0.5), which is a representative example. Generally, the photometry in a filter is uniform within one tile to within a few percent. The right column of Figure 5 shows the distribution of the Median Absolute Deviation (MAD) of the stellar photometry between KiDS and SDSS for the tiles in KiDS-North, demonstrating the photometric stability within survey tiles. The relatively poor photometry in u-band is due to the lack of photometric homogenization within a tile.

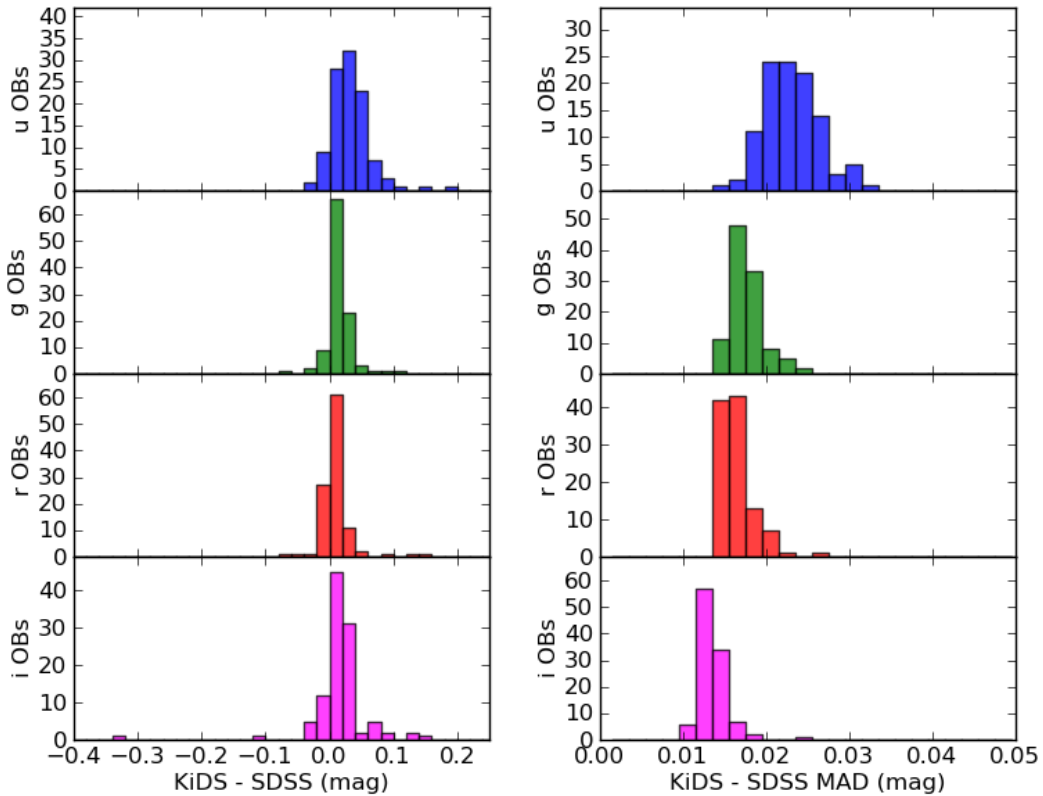


Figure 5: Photometric quality overview of KiDS-ESO-DR1 and KiDS-ESO-DR2 (all data contained in the multi-band catalogue). **Left:** distributions of the median photometric offsets for stars between the tiles in KiDS-North and SDSS DR8. **Right:** distributions of the Median Absolute Deviations of the photometric offsets for stars between the tiles in KiDS-North and SDSS DR8. In both columns the panels correspond to u, g, r, and i from top to bottom.

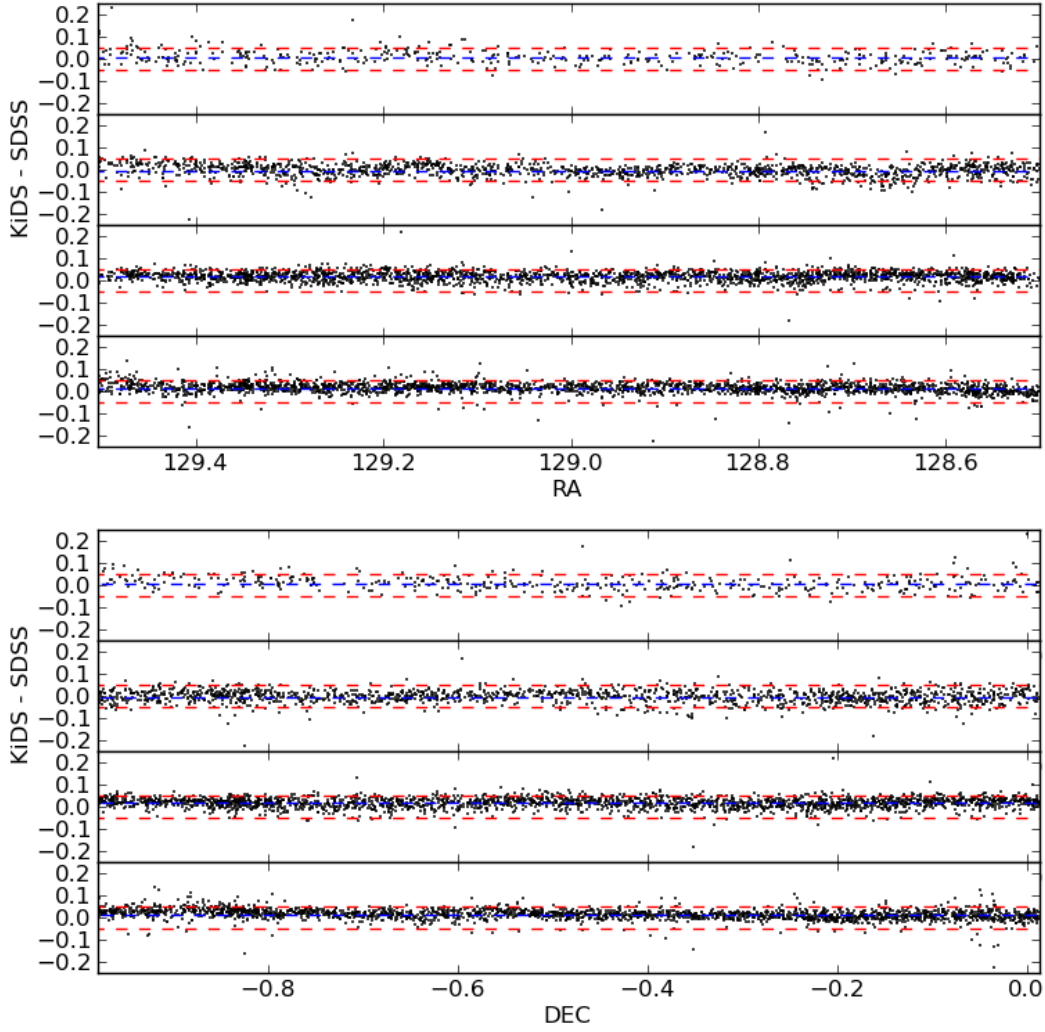


Figure 6: KiDS – SDSS DR8 magnitude offsets for (unmasked) stars in tile KiDS 129.0 -0.5 vs RA (top panel) and DEC (bottom panel), with the subpanels corresponding to u, g, r, and i, respectively. Each dot corresponds to a star, while the average indicated by a blue dashed line and with red dotted lines indicating +0.05 and -0.05 magnitudes.

### Color terms

The photometric calibration provided in KiDS-ESO-DR2 is in AB magnitudes in the instrumental system. Color-terms have been calculated with respect to the SDSS photometric system.

Aperture-corrected magnitudes taken from the multi-band catalogue, were matched to SDSS (DR8) PSF magnitudes of point-like sources. For each filter, the median offset to SDSS is first subtracted, rejecting tiles where this offset exceeds 0.1 mag in any of the g, r and i bands. The fit is done on all points from the remaining tiles. Figure 7 shows the photometric comparison and the following equations give the resulting color terms:

$$\begin{aligned}
 u_{\text{KiDS}} - u_{\text{SDSS}} &= (-0.050 \pm 0.002)(u_{\text{SDSS}} - g_{\text{SDSS}}), \\
 g_{\text{KiDS}} - g_{\text{SDSS}} &= (-0.052 \pm 0.002)(g_{\text{SDSS}} - r_{\text{SDSS}}), \\
 r_{\text{KiDS}} - r_{\text{SDSS}} &= (-0.033 \pm 0.002)(g_{\text{SDSS}} - r_{\text{SDSS}}), \\
 i_{\text{KiDS}} - i_{\text{SDSS}} &= (+0.012 \pm 0.002)(r_{\text{SDSS}} - i_{\text{SDSS}}).
 \end{aligned}$$

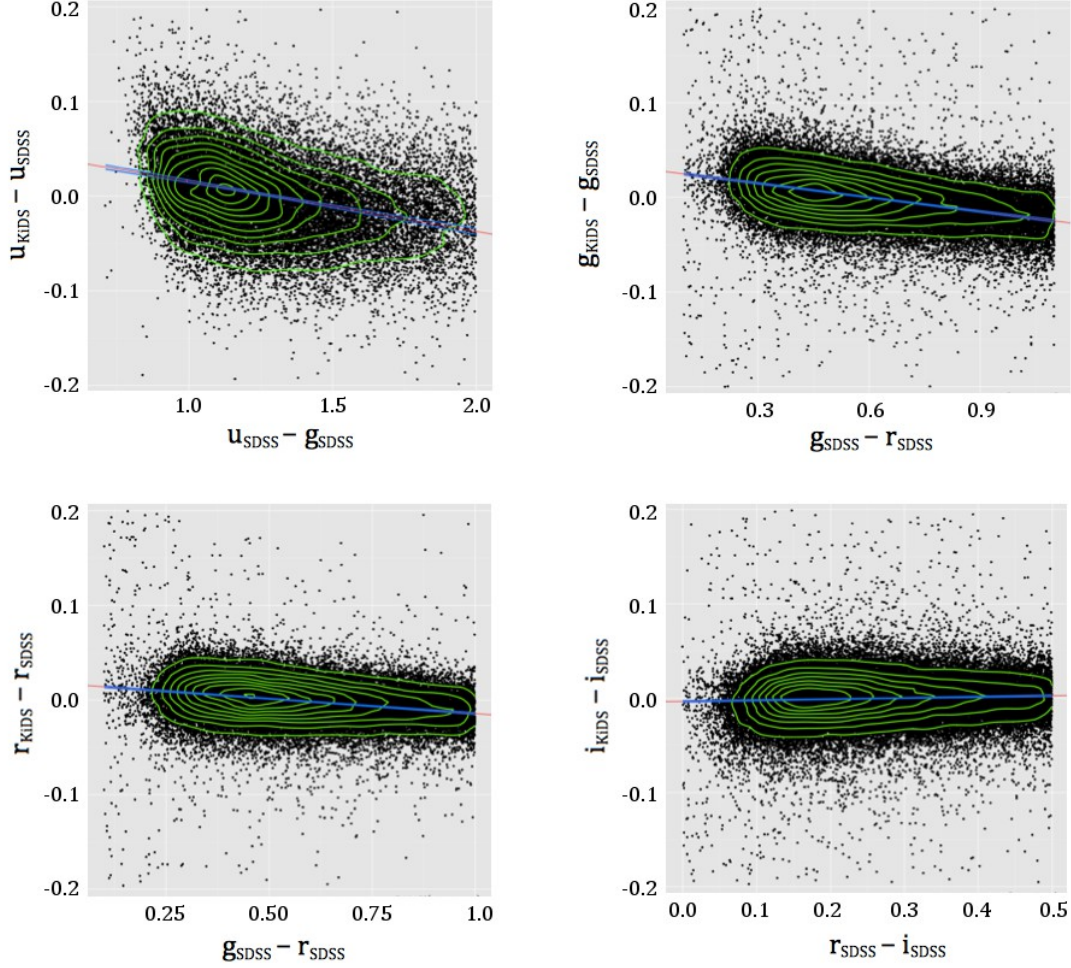


Figure 7: Derivation of color-terms of KiDS photometry w.r.t. the SDSS photometric system. The distribution of stars (black dots) is overlaid with contours (green) and fit by a linear relation (red line, with blue lines indicating the statistical uncertainty).

#### Astrometric quality

The accuracy of the absolute astrometry (“KiDS vs 2MASS”) is uniform over a coadd, with typical 2-dimensional (2-D) RMS of 0.31 arcsec in g, r, and i, and 0.25 arcsec in u. The lower RMS in u-band is most likely due to the fact that in this band on average brighter 2MASS sources are selected as reference sources. The accuracy of the relative astrometry (“KiDS vs KiDS”), measured by the 2-D positional residuals of sources between dithers, is also uniform across a single coadd. In Figure 8 the accuracy of this relative astrometry of all coadds is shown. The typical 2-D RMS is  $\sim 0.03$  arcsec in all filters, but with a larger scatter in u. The larger range in RMS in u-band is due to the smaller number of available reference sources.

#### Completeness and contamination

Contamination of the KiDS multi-band catalogue by spurious sources was analysed through a comparison of the overlap between KiDS-ESO-DR2 and the CFHT Legacy Survey (<http://www.cfht.hawaii.edu/Science/CFHLS/>), the main deeper survey overlapping with the current release (CFHTLS-W2, using their final data release T0007). For the analysis it is assumed that all KiDS sources not detected in CFHTLS-W2 are spurious. Since some fraction of real sources might be absent in the CFHTLS catalogues, the spurious fractions derived should be considered upper limits.

Figure 9 shows the spurious fractions derived from this comparison as function of magnitude (r-band  $MAG\_ISO$ ) and signal-to-noise (in a 2" aperture). When all sources in the catalogue are considered the fraction of spurious sources is estimated to be  $<5\%$  down to a very low SNR of  $\sim 5$  within a 2" aperture. Filtering sources based on masking information reduces this fraction to  $\sim 2\%$ , demonstrating that caution is required when using faint sources in masked regions. When

also sources with non-zero SExtractor detection flags are filtered out, the spurious fractions drops even further to  $\sim 1\%$ , yielding a very clean catalogue down to the detection limit.

An internal estimate of the completeness for KiDS-ESO-DR2 is provided per tile, based on the method of Garilli et al. 1999 (A&A, 342, 408). It determines the magnitude at which objects start to be lost in the source list because they are below the brightness threshold in the detection cell. The implementation is similar to La Barbera et al. (2010, MNRAS, 408, 1313). Estimates of the completeness obtained by comparison to deeper CFHTLS-W2 data are consistent with these internally derived values. The distributions of the 98% completeness magnitudes for all tiles are shown in Figure 8. Comparison with Figure 2 shows that the 98% completeness limits are typically  $\sim 1$  magnitude brighter than the limiting magnitude for g, r and i and  $\sim 1.3$  magnitudes brighter in u. For the completeness of the multi-band catalogue the values for the r-band of each tile apply.

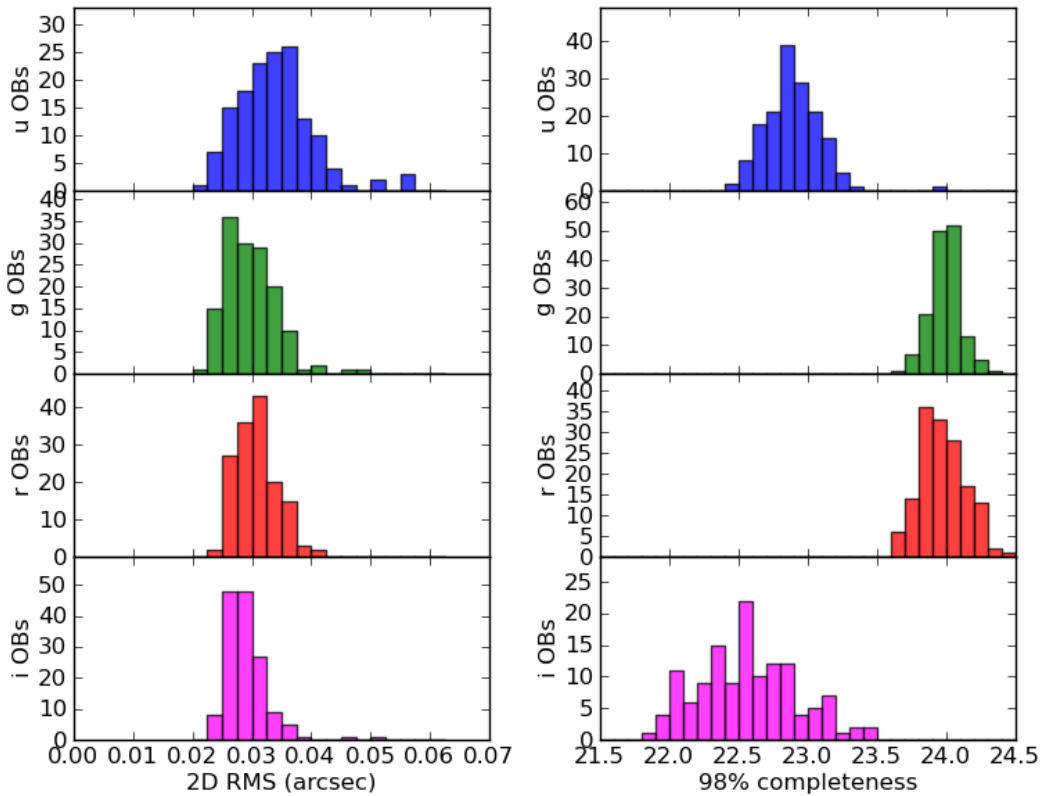


Figure 8: Overview of the astrometric quality and completeness of KiDS-ESO-DR1 and KiDS-ESO-DR2 (all data contained in the multi-band catalogue). **Left:** median relative astrometric offsets between the dithers in a coadd. **Right:** 98% completeness magnitude distributions for all tiles. In both columns the panels correspond to u, g, r, and i from top to bottom.

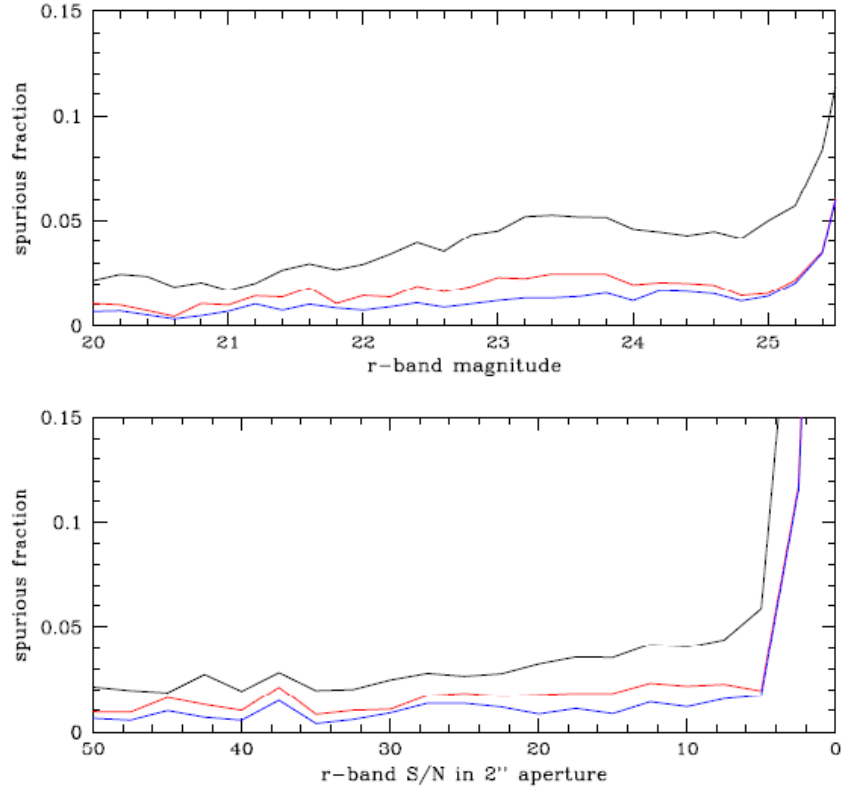


Figure 9: Spurious source contamination in the overlap between KiDS-ESO-DR2 and the CF-HTLS-W2 field (this corresponds to the KiDS tiles `KiDS_135.0_-1.5` and `KiDS_136.0_-1.5`). **Top:** spurious fraction vs. *r*-band magnitude (`MAG_ISO`). **Bottom:** spurious fraction vs. signal-to-noise in a 2'' aperture. The black line corresponds to all sources, while the red line excludes sources in masked areas, and the blue line excludes sources in masked areas and sources with a non-zero SExtractor flag.

## Known issues

### Scattered light and reflections

Some of the main issues in the early VST/OmegaCAM data are related to scattered light and reflections. Due to the open structure of the telescope, light from sources outside the field-of-view is often affecting the observations. This expresses itself in a number of ways:

- reflections: in some cases strong reflected light patterns are seen in the focal plane; these are caused by light from bright point sources outside the field-of-view and can occur in all filters. Some examples are shown in Figure 10a.
- vignetting by CCD masks: vignetting and scattering by the masks present at the corners of the focal plane array, and at the gaps between the rows of CCDs; this effect is particularly strong in *i*-band due to the bright conditions. The effect near the CCD gaps is largely corrected for, but in many cases the areas in the corners of the CCD array is strongly affected. Examples are shown in Figure 10b.
- extended background artifacts: related to the reflections mentioned before, this is mostly seen in *i*-band and probably caused by moonlight. An example is shown in Figure 10c.

Most of these effects are not (yet) corrected for in the current data processing, but strongly affected regions are included in the image masks provided in this data release and affected sources are flagged in the source lists.

Improvements to the telescope baffles that were installed in early 2014 should significantly improve scattered light suppression.

### Individual CCD issues

There are two issues related to individual CCDs that noticeably affect this data delivery:

- CCD 82: this CCD suffered from random gain jumps and related artifacts until its video board was replaced on June 2 2012. Artefacts as shown in Figure 10d are sometimes visible in the image stacks due to this problem. Photometry in this CCD can be used due to the cross-calibration with neighbouring CCDs in the dithered exposures, but part of the CCD is lost. These features are included in the image masks and affected sources are flagged.
- CCD 93: during a few nights in September 2011 (Early Science Time) one CCD was effectively dead due to a video cable problem. One observation included in this data delivery does not include this CCD: the i-band observation of KIDS\_341.2\_-32.1.

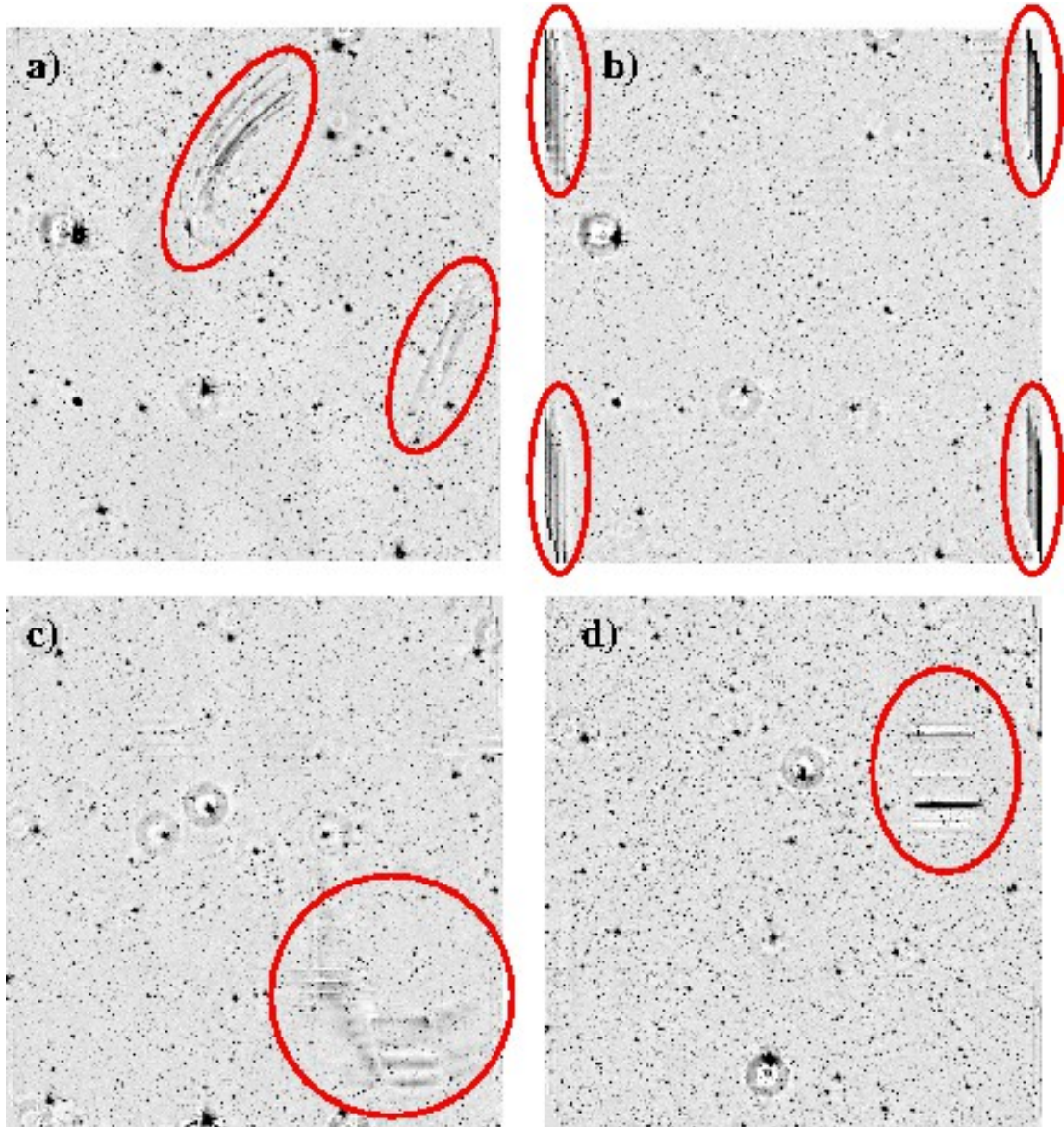


Figure 10: examples known issues in the VST/OmegaCAM data, highlighted by the red ellipses. **a)** light patterns caused by reflections and scattered light of bright sources outside the FOV. **b)** vignetting and scattering by CCD masks at the corners of the CCD array. **c)** extended background structures caused by scattering of moonlight. **d)** patterns caused by defective video board of CCD 82.

## Previous Releases

KiDS-ESO-DR1, with release number 1, precedes the current data release (KiDS-ESO-DR2), which is KiDS public release number 2.

Compared to KiDS-ESO-DR1 the current release adds 98 additional survey tiles, as well as a multi-band source catalogue encompassing the combined area of releases 1 and 2.

## Data Format

### Files Types

Table 5 lists the types of data products provided in this release, together with descriptions of the file types and naming conventions used.

The naming convention used for all data products is the following:

`KiDS_DR2.0_R.R_D.D_F_TTT.fits`,

where R.R and D.D are the RA and DEC of the tile center in degrees (J2000.0) with 1 decimal place, F is the filter (u, g, r, or i), and TTT is the data product type. The value of TTT for the different data products is given in column 4 of Table 5.

For example: the r-band stacked image of the tile “KIDS\_48.3-33.1” is called

`KiDS_DR2.0_48.3_-33.1_r_sci.fits`.

Data product	ESO product category name	File type	TTT
Calibrated, stacked images	SCIENCE.IMAGE	FITS image	sci
Weight frames	ANCILLARY.WEIGHTMAP	FITS image	wei
Masks	ANCILLARY.MASK	FITS image	msk
Single-band source lists	SCIENCE.SRCTBL	Binary FITS table	src
Multi-band catalogue data file	SCIENCE.MCATALOG	Binary FITS table	src

Table 5: data products and file types

### Format of coadded images

The final calibrated, coadded images have a uniform pixel scale of 0.2 arcsec. The pixel units are fluxes relative to the flux corresponding to magnitude = 0. This means that the effective zeropoint is equal to 0 and the magnitude  $m$  corresponding to a pixel value  $f$  is:

$$m = -2.5 \log_{10} f.$$

### Catalogue Columns

Table 6 lists the columns that are present in the single-band source lists provided in KiDS-ESO-DR2. A large number (27) of aperture fluxes, are provided to suit the needs of different users and allow interpolation to estimate e.g. aperture corrections. Only the columns for the smallest aperture (2 pixels, or 0.4 arcsec diameter) and the largest aperture (200 pixels, or 40 arcsec diameter) are listed in Table 6. Note: the label for the aperture of 28.5 pixels is FLUX\_APER\_28p5.

Table 7 lists the columns that are present in the multi-band source catalogue provided in KiDS-ESO-DR2. Measurements that are provided in each of the four filters are listed only once in the second part of Table 7, where <F> in the label is either 'U', 'G', 'R', or 'I' for the filters u, g, r and i.

Label	Format	Unit	Description
2DPHOT	J		Source classification
X_IMAGE	E	pixel	Object position along x
Y_IMAGE	E	pixel	Object position along y

Label	Format	Unit	Description
NUMBER	J		Running object number
CLASS_STAR	E		S-Extractor S/G classifier
FLAGS	J		Extraction flags
IMAFLAGS_ISO	J		FLAG-image flags OR'ed over the iso. profile
NIMAFLAG_ISO	J		Number of flagged pixels entering IMA-FLAGS_ISO
FLUX_RADIUS	E	pixel	Fraction-of-light radii
KRON_RADIUS	E	pixel	Kron apertures in units of A or B
FWHM_IMAGE	E	pixel	FWHM assuming a gaussian core
ISOAREA_IMAGE	J	pixel**2	Isophotal area above Analysis threshold
ELLIPTICITY	E		$1 - B\_IMAGE/A\_IMAGE$
THETA_IMAGE	E	deg	Position angle (CCW/x)
MAG_AUTO	E	mag	Kron-like elliptical aperture magnitude
MAGERR_AUTO	E	mag	RMS error for AUTO magnitude
ALPHA_J2000	D	deg	Right ascension of barycenter (J2000)
DELTA_J2000	D	deg	Declination of barycenter (J2000)
FLUX_APER_2	E	count	Flux vector within circular aperture of 2 pixels
...	...	...	...
FLUX_APER_200	E	count	Flux vector within circular aperture of 200 pixels
FLUXERR_APER_2	E	count	RMS error vector for flux within aperture of 2 pixels
...	...	...	...
FLUXERR_APER_200	E	count	RMS error vector for flux within aperture of 2 pixels
MAG_ISO	E	mag	Isophotal magnitude
MAGERR_ISO	E	mag	RMS error for isophotal magnitude
MAG_ISOCOR	E	mag	Corrected isophotal magnitude
MAGERR_ISOCOR	E	mag	RMS error for corrected isophotal magnitude
MAG_BEST	E	mag	Best of MAG_AUTO and MAG_ISOCOR
MAGERR_BEST	E	mag	RMS error for MAG_BEST
BACKGROUND	E	count	Background at centroid position
THRESHOLD	E	count	Detection threshold above background
MU_THRESHOLD	E	arcsec**(-2)	Detection threshold above background
FLUX_MAX	E	count	Peak flux above background
MU_MAX	E	arcsec**(-2)	Peak surface brightness above background
ISOAREA_WORLD	E	deg**2	Isophotal area above Analysis threshold
XMIN_IMAGE	J	pixel	Minimum x-coordinate among detected pixels
YMIN_IMAGE	J	pixel	Minimum y-coordinate among detected pixels
XMAX_IMAGE	J	pixel	Maximum x-coordinate among detected pixels
YMAX_IMAGE	J	pixel	Maximum y-coordinate among detected pixels
X_WORLD	D	deg	Barycenter position along world x axis
Y_WORLD	D	deg	Barycenter position along world y axis
XWIN_IMAGE	E	pixel	Windowed position estimate along x
YWIN_IMAGE	E	pixel	Windowed position estimate along y
X2_IMAGE	D	pixel**2	Variance along x
Y2_IMAGE	D	pixel**2	Variance along y
XY_IMAGE	D	pixel**2	Covariance between x and y
X2_WORLD	E	deg**2	Variance along X-WORLD (alpha)
Y2_WORLD	E	deg**2	Variance along Y-WORLD (delta)

Label	Format	Unit	Description
XY_WORLD	E	deg**2	Covariance between X-WORLD and Y-WORLD
CXX_IMAGE	E	pixel**(-2)	Cxx object ellipse parameter
CYY_IMAGE	E	pixel**(-2)	Cyy object ellipse parameter
CXY_IMAGE	E	pixel**(-2)	Cxy object ellipse parameter
CXX_WORLD	E	deg**(-2)	Cxx object ellipse parameter (WORLD units)
CYY_WORLD	E	deg**(-2)	Cyy object ellipse parameter (WORLD units)
CXY_WORLD	E	deg**(-2)	Cxy object ellipse parameter (WORLD units)
A_IMAGE	D	pixel	Profile RMS along major axis
B_IMAGE	D	pixel	Profile RMS along minor axis
A_WORLD	E	deg	Profile RMS along major axis (WORLD units)
B_WORLD	E	deg	Profile RMS along minor axis (WORLD units)
THETA_WORLD	E	deg	Position angle (CCW/world-x)
THETA_J2000	E	deg	Position angle (east of north) (J2000)
ELONGATION	E	deg	A_IMAGE/B_IMAGE
ERRX2_IMAGE	E	pixel**2	Variance of position along x
ERRY2_IMAGE	E	pixel**2	Variance of position along y
ERRXY_IMAGE	E	pixel**2	Covariance of position between x and y
ERRX2_WORLD	E	deg**2	Variance of position along X-WORLD (alpha)
ERRY2_WORLD	E	deg**2	Variance of position along Y-WORLD (delta)
ERRXY_WORLD	E	deg**2	Covariance of position X-WORLD/Y-WORLD
ERRCXX_IMAGE	E	pixel**(-2)	Cxx error ellipse parameter
ERRCYY_IMAGE	E	pixel**(-2)	Cyy error ellipse parameter
ERRCXY_IMAGE	E	pixel**(-2)	Cxy error ellipse parameter
ERRCXX_WORLD	E	deg**(-2)	Cxx error ellipse parameter (WORLD units)
ERRCYY_WORLD	E	deg**(-2)	Cyy error ellipse parameter (WORLD units)
ERRCXY_WORLD	E	deg**(-2)	Cxy error ellipse parameter (WORLD units)
ERRA_IMAGE	E	pixel	RMS position error along major axis
ERRB_IMAGE	E	pixel	RMS position error along minor axis
ERRA_WORLD	E	deg	World RMS position error along major axis
ERRB_WORLD	E	deg	World RMS position error along minor axis
ERRTHETA_IMAGE	E	deg	Error ellipse pos. angle (CCW/x)
ERRTHETA_WORLD	E	deg	Error ellipse pos. angle (CCW/world-x)
ERRTHETA_J2000	E	deg	J2000 error ellipse pos. angle (east of north)
FWHM_WORLD	E	deg	FWHM assuming a gaussian core
ISO0	J	pixel**2	Isophotal area at level 0
ISO1	J	pixel**2	Isophotal area at level 1
ISO2	J	pixel**2	Isophotal area at level 2
ISO3	J	pixel**2	Isophotal area at level 3
ISO4	J	pixel**2	Isophotal area at level 4
ISO5	J	pixel**2	Isophotal area at level 5
ISO6	J	pixel**2	Isophotal area at level 6
ISO7	J	pixel**2	Isophotal area at level 7
SLID	K		Source list ID
SID	K		Source ID within the source list
HTM	K		Hierarchical Triangular Mesh (level 25)
FLAG	K		Not used

Table 6: columns provided in the KiDS-ESO-DR2 single-band source lists

Label	Format	Unit	Description
<b>Measurements based on r-band detection image</b>			
ID	23A		Source identifier
RAJ2000	D	deg	Right ascension
DECJ2000	D	deg	Declination
SG2DPHOT	K		Star/galaxy separation
A	D	pixel	Linear semi major axis
B	D	pixel	Linear semi minor axis
CLASS_STAR	E		S-Extractor star/galaxy classifier
ELLIPTICITY	E		Ellipticity
KRON_RADIUS	E	pixel	Kron-radius used for MAG_AUTO
POSANG	E	deg	Position angle
SEQNR	K		r-band sequence number
<b>Measurements provided for each filter</b>			
FLUXERR_APER_100_<F>	E	count	flux error in 100 pixel aperture
FLUXERR_APER_10_<F>	E	count	flux error in 10 pixel aperture
FLUXERR_APER_14_<F>	E	count	flux error in 14 pixel aperture
FLUXERR_APER_25_<F>	E	count	flux error in 25 pixel aperture
FLUXERR_APER_40_<F>	E	count	flux error in 40 pixel aperture
FLUXERR_APER_4_<F>	E	count	flux error in 4 pixel aperture
FLUXERR_APER_6_<F>	E	count	flux error in 6 pixel aperture
FLUXERR_APERCOR_10_<F>	E	count	corrected flux error from 10 pixel aperture
FLUXERR_APERCOR_14_<F>	E	count	corrected flux error from 14 pixel aperture
FLUXERR_APERCOR_25_<F>	E	count	corrected flux error from 25 pixel aperture
FLUXERR_APERCOR_4_<F>	E	count	corrected flux error from 4 pixel aperture
FLUXERR_APERCOR_6_<F>	E	count	corrected flux error from 6 pixel aperture
FLUX_APER_100_<F>	E	count	flux in 100 pixel aperture
FLUX_APER_10_<F>	E	count	flux in 10 pixel aperture
FLUX_APER_14_<F>	E	count	flux in 14 pixel aperture
FLUX_APER_25_<F>	E	count	flux in 25 pixel aperture
FLUX_APER_40_<F>	E	count	flux in 40 pixel aperture
FLUX_APER_4_<F>	E	count	flux in 4 pixel aperture
FLUX_APER_6_<F>	E	count	flux in 6 pixel aperture
FLUX_APERCOR_10_<F>	E	count	corrected flux from 10 pixel aperture
FLUX_APERCOR_14_<F>	E	count	corrected flux from 14 pixel aperture
FLUX_APERCOR_25_<F>	E	count	corrected flux from 25 pixel aperture
FLUX_APERCOR_4_<F>	E	count	corrected flux from 4 pixel aperture
FLUX_APERCOR_6_<F>	E	count	corrected flux from 6 pixel aperture
FLUX_RADIUS_<F>	E	pixel	S-Extractor FLUX_RADIUS
FWHM_IMAGE_<F>	E	pixel	S-Extractor FWHM_IMAGE
FLAG_<F>	J		S-Extractor extraction flag
IMAFLAGS_ISO_<F>	J		mask flag
MAGERR_AUTO_<F>	E	mag	error in MAG_AUTO
MAGERR_ISO_<F>	E	mag	error in MAG_ISO
MAG_AUTO_<F>	E	mag	MAG_AUTO
MAG_ISO_<F>	E	mag	MAG_ISO
NIMAFLAGS_ISO_<F>	J		number of masked pixels
ISOAREA_IMAGE_<F>	J	pixel**2	isophotal aperture
XPOS_<F>	E	pixel	X pixel position
YPOS_<F>	E	pixel	Y pixel position

Table 7: columns provided in the KiDS-ESO-DR2 multi-band catalogue.

## Acknowledgements

The following acknowledgment is valid at the moment of writing this document. For an up-to-date version, please visit the following webpage: <http://kids.strw.leidenuniv.nl/DR2/acknowledgements.php>

Users of data from this release should cite “de Jong et al. (2013, ExA 35, 25)”.

Please use the following statement in your articles when using these data:

*Based on data products from observations made with ESO Telescopes at the La Silla Paranal Observatory under programme IDs 177.A-3016, 177.A-3017 and 177.A-3018, and on data products produced by Target/OmegaCEN, INAF-OACN, INAF-OAPD and the KiDS production team, on behalf of the KiDS consortium. OmegaCEN and the KiDS production team acknowledge support by NOVA and NWO-M grants. Members of INAF-OAPD and INAF-OACN also acknowledge the support from the Department of Physics & Astronomy of the University of Padova, and of the Department of Physics of Univ. Federico II (Naples).*